Demography and Diffusion in Epidemics: Malaria and Black Death Spread

Article *in* Acta Biotheoretica · September 2010

DOI: 10.1007/s10441-010-9103-z · Source: PubMed

6 authors, including:

Jean Gaudart
Aix-Marseille Université
286 PUBLICATIONS **4,003** CITATIONS
SEE PROFILE

Mustapha Rachdi
Université Grenoble Alpes
99 PUBLICATIONS **765** CITATIONS
SEE PROFILE

Jules Waku
University of Yaounde I
17 PUBLICATIONS **107** CITATIONS
SEE PROFILE

Jacques Demongeot
Université Grenoble Alpes
488 PUBLICATIONS **6,465** CITATIONS
SEE PROFILE

Acta Biotheor (2010) 58:277–305
DOI 10.1007/s10441-010-9103-z

REGULAR ARTICLE

Demography and Diffusion in Epidemics: Malaria and Black Death Spread

J. Gaudart · M. Ghassani · J. Mintsa · M. Rachdi · J. Waku · J. Demongeot

Received: 23 June 2010 / Accepted: 28 June 2010 / Published online: 13 August 2010

Abstract The classical models of epidemics dynamics by Ross and McKendrick have to be revisited in order to incorporate elements coming from the demography (fecundity, mortality and migration) both of host and vector populations and from the diffusion and mutation of infectious agents. The classical approach is indeed dealing with populations supposed to be constant during the epidemic wave, but the presently observed pandemics show duration of their spread during years imposing to take into account the host and vector population changes as well as the transient or permanent migration and diffusion of hosts (susceptible or infected), as well as vectors and infectious agents. Two examples are presented, one concerning the malaria in Mali and the other the plague at the middle-age.

Keywords Epidemics modelling · Contagious diseases · Endemic state · Black Death · Demographic dynamics · Reaction–diffusion

J. Gaudart
LERTIM, EA 3283, Faculty of Medicine, Aix-Marseille University,
27 Bd Jean Moulin, 13385 Marseille Cedex 5, France
e-mail: jean.gaudart@univmed.fr

M. Ghassani · J. Mintsa · M. Rachdi · J. Waku · J. Demongeot (✉)
TIMC-IMAG, AGIM3, UMR CNRS 5525, Faculty of Medicine of Grenoble,
University J. Fourier, 38700 La Tronche, France
e-mail: Jacques.Demongeot@imag.fr

M. Ghassani
e-mail: Mohamad.Ghassani@imag.fr

J. Mintsa
e-mail: Julie.Mintsa@imag.fr

M. Rachdi
e-mail: Mustapha.Rachdi@imag.fr

J. Waku
e-mail: Jules.Waku@imag.fr

1 Introduction

Major advances in epidemics modelling have been done recently by introducing demographic aspects (i.e. consideration of host and vector populations whose global size changes during both epidemic and endemic histories) as well as spatial aspects about host, vector or infectious agent spread or genetic change (Gaudart et al. 2010). Mathematical tools corresponding to these improvements have been recently introduced making the classical models more realistic, hence more convenient for prediction and anticipation (like vaccination or other measures of public health limiting the contagion). As examples of application, the dynamics of two infectious diseases will be studied: the malaria endemics in the south of Mali, and a well-known historic plague epidemics, the Black Death (1347–1352), which occurred at the Middle Age and whose demographic and socio-economic consequences were dramatic: about 25 million deaths in Europe, and 25 million in Asia (Prentice and Rahalison 2007).

Despite remaining simple, the models presented in this paper account qualitatively for the morphology of the endemic spatial distribution and of the epidemic front waves. Perspectives will be drawn concerning present epidemic risks, in which a model like those well retro-predicting the Black Death episode could be "mutatis mutandis" useful to predict the dynamical behavior of future epidemics.

2 Classical Epidemiology: The Ross-McKendrick Model

After the first historical model by Bernoulli (Bernoulli 1760; Zeeman 1993; Dietz and Heesterbeek 2000, 2002) proposed for explaining the small pox dynamics, many discussions occurred about the efficacy of firstly the inoculation and secondly the vaccination (d'Alembert 1761; Murray 1763; L'Épine 1764; Lambert 1772; May 1770; Trembley 1796). In the model princeps, the population is divided into susceptibles (not yet been infected) and immunes (immunized for the rest of their life after one infection), and the two corresponding variables are $u(a)$, the probability for a newborn individual of being susceptible and alive at age a, and $w(a)$, the probability of being immune and alive at age a. Ross (1916), McKendrick (1925), Kermack and McKendrick (1932, 1933) proposed a model called Susceptible-Infectives-Recovered with immunity (SIR) model, with equations:

$$\begin{aligned} \frac{dS}{dt} &= \delta S + \delta I + (\delta + \gamma)R - \beta SI - \delta S \\ \frac{dI}{dt} &= \beta SI - (\delta + v)I \\ \frac{dR}{dt} &= vI - (\delta + \gamma)R, \end{aligned} \tag{1}$$

where S (resp. I, R) denotes the size of Susceptible (Infective, Recovered) population with $S + I + R = N$, β (resp. δ, γ, v) being the contagion (resp. death/birth, loss of resistance, immunization) rate (Fig. 1) (May and Anderson 1984). The epidemic parameter $R0 = \beta N/(v + \delta)$ is the mean number of secondary infecteds by

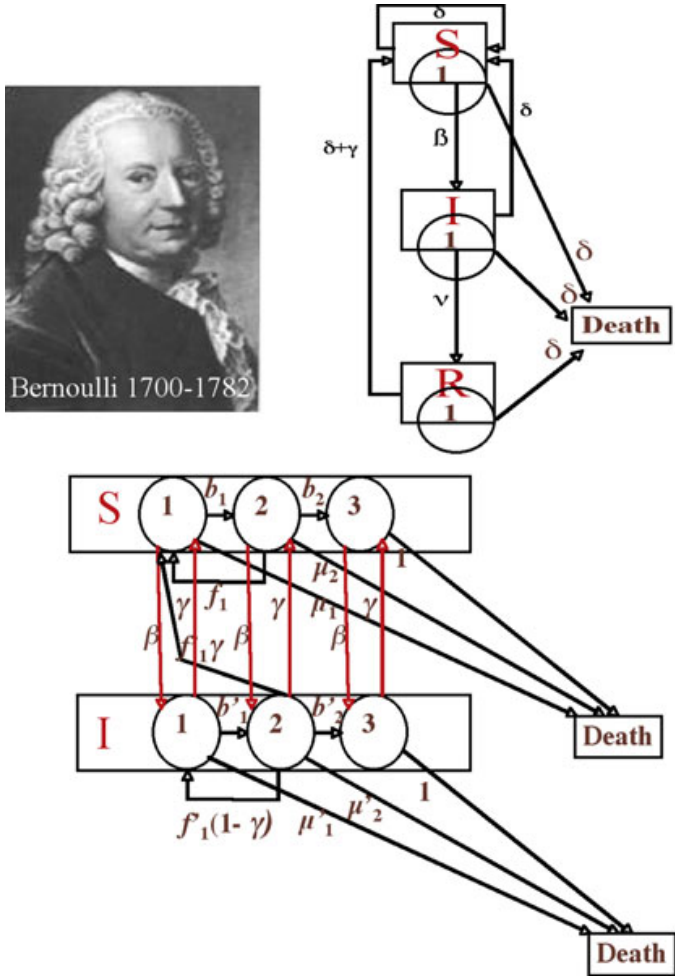

Fig. 1 Picture of D. Bernoulli (*top left*); interaction digraphs of the Ross-McKendrick model with 1 (*top right*) and extended with 3 (*bottom*) age classes, with identical β_i's and γ_i's and no fecundity in elderly classes S_3 and I_3

one primary infective and predicts, if it is greater than 1, the occurrence of an epidemic wave. By defining age classes denoted S_i, I_i and R_i ($i = 1, \ldots, n$) in each subpopulation of S, I and R, we have at any stationary state (S^*, I^*, R^*):

$$u^*(i) = \frac{S_i^*}{S_1^*}, v^*(i) = \frac{I_i^*}{I_1^*}, w^*(i) = \frac{R_i^*}{R_1^*} \tag{2}$$

The relationships (2) between the probabilities for a newborn individual of being alive and either susceptible, infected or immune at age i make the link between the Bernoulli and the Ross-McKendrick models, but the weakness of the latter still resides in many insufficiencies and approximations:

- when the population sizes of either susceptibles or infectives tend to be very large, the quadratic term SI has to be replaced by a Michaelian saturation term $SI/((k + S)(k' + I))$
- the immunized infectives or healthy carriers are neglected
- the total population size is supposed to be constant, the fecondity just equalling the natural mortality. The Bernoulli model taken implicitly into account the fecundity, and explicitly the natural mortality. The model by d'Alembert improved the Bernoulli's one by distinguishing the specific mortality due to the infectious disease from the natural one, being more widely applicable than the model by Bernoulli which was restricted to immunizing infections. In d'Alembert's method

the only task was to calculate the survival function after eliminating a particular cause of death (the infectious disease), but the Bernoulli's approach provided much more insight for a mechanistic interpretation of infectious disease data

- variables and parameters do not depend on space (no migration nor population displacement)
- parameters do not depend on time (no genetic adaptation of infectious agent or human population, even very slow compared to the fast dynamics of epidemics).

We will now improve the Ross-McKendrick model by trying to partly compensate these defects. We will first introduce the age classes into the host population to account for its growth, the space dependence to account for the host and vector population migration, and eventually propose to take into account the genetic changes in all concerned populations before presenting examples of application and perspectives.

3 Introduction of Demographic Dynamics

3.1 Introduction of Age Classes

By introducing age classes, we add new demographic parameters as the fecundity rate f_i, equal to the mean number of offsprings a person in age class i is sending in age class 1 between t and $t + dt$, and the survival (resp. death) rate b_i (resp. μ_i) equal to the probability to survive from age i to age $i + 1$ (resp. to die at age i) between t and $t + dt$. When the biological age is defined by physiology of cells and tissues (Demongeot 2009) with the possibility to remain in the same age between t and $t + dt$ (despite of the fact that the chronological age is increasing of dt), then $\beta + b_i + \mu_i < 1$. The equations of the extendend Ross-McKendrick model correspond to 2 age classes are the following (cf. Fig. 1, by reducing the class number from 3 to 2):

$$\begin{aligned}
\frac{dS_1}{dt} &= -(\beta_{11}I_1 + \beta_{12}I_2)S_1 - b_1S_1 + \gamma_1 I_1 + f_1^S S_1 \\
&\quad + f_2^S S_2 + (1-\theta_1)f_1^I I_1 + (1-\theta_2)f_2^I I_2 - \mu_1 S_1 \\
\frac{dS_2}{dt} &= -(\beta_{21}I_1 + \beta_{22}I_2)S_2 + b_1S_1 + \gamma_2 I_2 - \mu_2 S_2 \\
\frac{dI_1}{dt} &= (\beta_{11}I_1 + \beta_{12}I_2)S_1 - b_1'I_1 - \gamma_1 I_1 + \theta_1 f_1^1 I_1 + \theta_2 f_2^1 I_2 - \mu_1' I_1 \\
\frac{dI_2}{dt} &= (\beta_{21}I_1 + \beta_{22}I_2)S_2 + b_1'I_1 - \gamma_2 I_2 - \mu_2' I_2
\end{aligned} \tag{3}$$

Herein μ'_i incorporates the mortality rate due to the disease, β_{ji} is the "efficient contagion rate" of susceptible S_j by infective I_i, $1/\gamma_i$ is the duration of the infective stage, f_i^z, with $i = 1,2$ and $z = S, I$, denote fertility rates satisfying $0 \leq f_i^I \leq f_i^S$, and finally $0 \leq \theta_1, \theta_2 \leq 1$ are the probabilities of vertical transmission. To be more precise in introducing the age classes, in particular with the biological age, we have

before to recall the classical models used for modelling the population growth (Doliger 2006; Demongeot 2009).

3.2 Leslie Model

The population growth has been modelled by Leslie (Leslie 1945) using the "age pyramid" vector $x(t) = (x_i(t))_{i=1,\ldots,n}$, where $x_i(t)$ represents the size of the age class i at time t, with i ranging from the birth age 1 to the maximal death age n, whose discrete dynamics is governed by the matrix equation:

$$x(t) = Lx(t-1), \tag{4}$$

$$\text{where } L = \left(l_{ij}\right) = \begin{pmatrix} f_1 & f_2 & f_3 & \ldots & \ldots & f_n \\ b_1 & 0 & 0 & \ldots & \ldots & 0 \\ 0 & b_2 & 0 & \ldots & \ldots & 0 \\ \ldots & & & & & \\ \ldots & & & & & \\ 0 & 0 & 0 & \ldots & b_{n-1} & 0 \end{pmatrix} \tag{5}$$

and where $b_i = 1 - \mu_i \leq 1, \forall\, i = 1, \ldots, n$, is the survival probability between ages i and $i + 1$ and f_i is the fecundity at age i (i.e. the mean number of offsprings from an individual at age i).

The dynamical stability for the L^2 distance between the stationary age pyramid w and the current age pyramid is related to $|\lambda - \lambda'|$, the modulus of the difference between the dominant and sub-dominant eigenvalues of L, namely $\lambda = e^r$ and λ' (where r is the Malthusian growth rate), where w is the eigenvector of L corresponding to λ. The dynamical stability for the Kullback distance to the stationary distribution of the probabilities that the mother of a newborn be in age i, is related to the population entropy H (Demongeot and Demetrius 1989).

3.3 Usher Model

The possibility to remain in the same biological age (corresponding to an increase of the longevity) or to pass over a biological age state (corresponding to an acceleration of ageing) between t and $t + dt$ has been modelled by Usher (Usher 1969) using the vector $x(t)$, whose discrete dynamics is ruled by the matrix equation:

$$x(t) = Ux(t-1), \tag{6}$$

$$\text{where } U = \left(u_{ij}\right) = \begin{pmatrix} f_1 + \alpha_1 & f_2 & f_3 & \ldots & f_{n-1} & f_n \\ \beta_1 & \alpha_2 & 0 & \ldots & \ldots & 0 \\ \gamma_1 & \beta_2 & \alpha_3 & \ldots & \ldots & 0 \\ \ldots & & & & & \\ 0 & 0 & 0 & \ldots & \alpha_{n-1} & 0 \\ 0 & 0 & 0 & \ldots & \beta_{n-1} & \alpha_n \end{pmatrix} \tag{7}$$

and where α_i (respectively β_i and γ_i) is the probability to remain in state i (respectively to go to state $(i + 1)$ and $(i + 2)$) between times t and $t + 1$, with $\alpha_i + \beta_i + \gamma_i = 1 - \mu_i \leq 1, \forall\, i = 1,\ldots,n$.

Like in the Leslie model of the previous Section, the dynamical stability for the L^2 distance between the stationary age pyramid w and the current age pyramid is linked to $|\lambda - \lambda'|$.

3.4 Mathematical Properties

Let us suppose that the last fecundity parameter f_n is strictly positive (which is for example the case for both host and vector populations, if the last age class keeps at least one fertile individual), then because the subdiagonal is supposed to be strictly positive, L and U are irreducible and nonnegative. Then from the Frobenius' theorem, L and U have a strictly positive, simple dominant eigenvalue λ, with an associated strictly positive eigenvector (stable age pyramid). The population is constant (resp. in explosion, in extinction) if the Malthusian parameter r satisfies: $r = \mathrm{Log}\lambda = 0$ (resp. >0, <0). For example, let us consider the model with two age classes both for hosts and vectors, whose dynamics is driven by Eq. 3 and interaction graph is given in the case of 3 age classes in Fig. 1. Let us denote $s_i = kS_i$ and $i_i = kI_i$. Various possibilities of demographic evolution and stability of the endemic state can be observed depending on the set of values fixed for the model parameters:

(1) ${f_2}^S = 499k/100$, ${f_2}^I = 0.2k$, $b_1 = 98k/96$, ${b'}_1 = k$, $\mu_1 = {\mu'}_1 = 0$, $\mu_2 = 49k/100$, ${\mu'}_2 = 4k/5$, $\beta_{11} = 4k^2/100$, $\gamma_1 = k/5$, $\beta_{22} = \beta_{12} = \beta_{21} = 0$, $\gamma_2 = 0$. Then, if $k = 1$, we have:

$$\begin{aligned}
\frac{dS_1}{dt} &= (20 - 4S_1)I_I/100 - 98S_1/100 + 499S_2/100 \\
\frac{dS_2}{dt} &= 98S_1/100 - 49S_2/100 \\
\frac{dI_1}{dt} &= 4I_1S_1/100 - I_1/5 - 4I_1/5 + 0.2I_2 \\
\frac{dI_2}{dt} &= 4I_I/5 - 4I_2/5
\end{aligned} \tag{8}$$

The two stationary points are denoted by $(s_1{*}, s_2{*}, i_1{*}, i_2{*}) = (0, 0, 0, 0)$ and $(s_1{**}, s_2{**}, i_1{**}, i_2{**}) = (20, 40, 15, 15)$ and they are both locally unstable. It is easily proved by calculating the Jacobian matrix J of the system (8) at the second endemic state and searching for roots of its characteristic polynomial. For the second stationary point, we have:

$$J - \lambda I \approx \begin{pmatrix} -1.6 - \lambda & 5 & -0.8 & 0 \\ 1 & -0.5 - \lambda & 0 & 0 \\ 0.6 & 0 & -0.2 - \lambda & 0.2 \\ 0 & 0 & 0.8 & -0.8 - \lambda \end{pmatrix}$$

Its characteristic polynomial P satisfies:

$$P(\lambda) = (-0.8-\lambda)[(-0.2-\lambda)[(-0.5-\lambda)(-1.6-\lambda)-5]-0.48(0.5+\lambda)] - 0.16[(-0.5-\lambda)(-1.6-\lambda)-5]$$

$P(0) > 0$ and $P(\infty) > 0$, then $\lambda > 0$

$P(1) < 0$, then $\lambda > 1$

$$P(\lambda) = (-0.8-\lambda)[-\lambda^3 + 1.9\lambda^2 + 4.94\lambda + 0.6] - 0.16\lambda^2 - 0.336\lambda + 0.672$$
$$= \lambda^4 - 1.1\lambda^3 - 3.42\lambda^2 - 4.552\lambda - 0.48 - 0.16\lambda^2 - 0.336\lambda + 0.672$$
$$= \lambda^4 - 1.1\lambda^3 - 3.58\lambda^2 - 5.188\lambda + 0.192$$

$P'(\lambda) = 4\lambda^3 - 3.3\lambda^2 - 7.16\lambda - 5.188$, $P''(\lambda) = 12\lambda^2 - 6.6\lambda - 7.16$,

$P'''(\lambda) = 24\lambda - 6.6$

From the endemic state, the population grows with a Malthusian parameter greater than 1 (on Fig. 2, the dominant eigenvalue λ is greater than 3), then N is not constant and the Ross-McKendrick framework is no more available.

(2) ${f_2}^S = 109k/100$; ${f_2}^I = 0.2k$; $b_1 = 98k/96$; $b'_1 = k$; $\mu_1 = \mu'_1 = 0$; $\mu_2 = 49k/100$; $\mu'_2 = 4k/5$; $\beta_{11} = 4k^2/100$; $\gamma_1 = k/5$; $\beta_{22} = \beta_{12} = \beta_{21} = 0$; $\gamma_2 = 0$. Then, if $k = 1$:

$$\begin{aligned}
\frac{dS_1}{dt} &= (20 - 4S_1)I_1/100 - 98S_1/100 + 109S_2/100 \\
\frac{dS_2}{dt} &= 98S_1/100 - 49S_2/100 \\
\frac{dI_1}{dt} &= 4S_1I_1/100 - I_1/5 - 4I_1/5 + 0.2I_2 \\
\frac{dI_2}{dt} &= 4I_1/5 - 4I_2/5
\end{aligned} \tag{9}$$

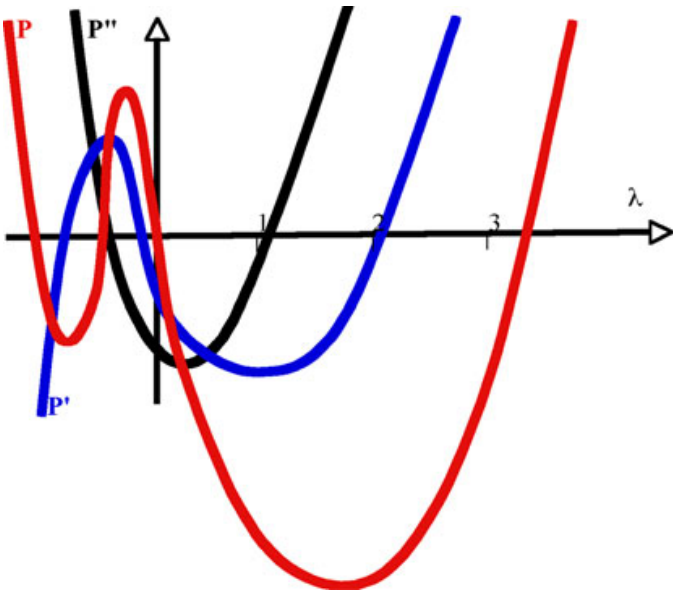

Fig. 2 Graphs of the functions $P(\lambda)$, $P'(\lambda)$ and $P''(\lambda)$

The characteristic polynomial P of the endemic state (s_1**, s_2**, i_1**, i_2**) = (20, 40, 2, 2) of the system (9) satisfies:

$$P(\lambda) = (-0.8-\lambda)[(-1.8-\lambda)[(-0.5-\lambda)(-1-\lambda)-1]-0.05(0.5+\lambda)] \\ -0.16[(-0.5-\lambda)(-1-\lambda)-1]$$

Then $P(0) < 0$ and $P(\infty) > 0$, ensuring that the dominant eigenvalue λ is strictly positive, and $P(1) > 0$, then $\lambda < 1$. The endemic state is unstable and all populations are in extinction.

(3) ${f_2}^S = k$; ${f_2}^I = 3k/4$; $b_1 = b'_1 = 3k/4$; $\mu_1 = \mu'_1 = 0$; $\mu_2 = \mu'_2 = k$; $\beta_{11} = k^2/4$; $\gamma_1 = k/4$; $\beta_{22} = \beta_{12} = \beta_{21} = 0$; $\gamma_2 = 0$.

Then, if $k = 1$:

$$\begin{aligned} \frac{dS_1}{dt} &= (1-S_1)I_1/4 - 9S_1/16 + S_2 \\ \frac{dS_2}{dt} &= 9S_1/16 - S_2 \\ \frac{dI_1}{dt} &= S_1I_1/4 - I_1/4 - 9I_1/16 + 3I_2/4 \\ \frac{dI_2}{dt} &= 9I_1/16 - I_2 \end{aligned} \tag{10}$$

The characteristic polynomial P of the endemic state (s_1**, s_2**, i_1**, i_2**) = (1/4, 9/64, 0, 0) of the system (10) satisfies:

$$16^4P(\lambda) = (-16-16\lambda)[(-12-16\lambda)[(-16-16\lambda)(-9-16\lambda)-144] \\ -108[(-9-16\lambda)(-16-16\lambda)-144]$$

Then $P(0) = 0$, $P(\infty) > 0$ and $P(x) > 0$, if $x > 0$, ensuring that the dominant eigenvalue λ is equal to 0. All populations are locally stable only in the Lyapunov sense, but are asymptotically unstable.

(4) ${f_2}^S = k/2$; ${f_2}^I = 0$; $b_1 = b'_1 = 2k/3$; $\mu_1 = \mu'_1 = 0$; $\mu_2 = \mu'_2 = k$; $\beta_{11} = k^2/2$; $\gamma_1 = k/2$; $\beta_{22} = \beta_{12} = \beta_{21} = 0$; $\gamma_2 = 0$. Then, if $k = 1$:

$$\begin{aligned} \frac{dS_1}{dt} &= (1-S_1)I_1/2 - S_1/3 + S_2/2 \\ \frac{dS_2}{dt} &= S_1/3 - S_2 \\ \frac{dI_1}{dt} &= S_1I_1/2 - I_1/2 - I_1/3 \\ \frac{dI_2}{dt} &= I_1/3 - I_2 \end{aligned} \tag{11}$$

The characteristic polynomial P of the endemic state (s_1**, s_2**, i_1**, i_2**) = (2/3, 2/9, 2/3, 2/9) of the system (11) satisfies:

$$\begin{aligned} 6^4 P(\lambda) &= (-6-6\lambda)[(-216\lambda^3 - 408\lambda^2 - 294\lambda - 54] \\ &= 1296\lambda^4 + 3774\lambda^3 + 4212\lambda^2 + 2088\lambda + 324 \end{aligned}$$

Then $P(0) > 0$, $P(\infty) > 0$ and $P(x) > 0$, if $x > 0$, ensuring that the dominant eigenvalue λ is strictly negative. The endemic state is locally stable.

4 Introduction of a Spatial Dynamics

The introduction of the space in Ross-McKendrick models can be made through stochastic spatial Markovian or renewal models (Demongeot and Fricot 1986), or deterministic Partial Differential Equations (PDE) in which the diffusion of hosts or vectors is modelled by the Laplacian operator Δ or possibly the d'Alembertian $\Box$, when some sub-populations can present an accelerated ageing (Demongeot 2009). These models are called SIGR with Diffusion (SIGRD) (de Magny et al. 2005). The Bankoumana model is a double SIGRD model (Gaudart et al. 2007, 2009, 2010) whose PDE equations have spatial initial conditions essentially determined by the spawning zones of mosquitos in backwater places.

These zones are depending on the rainfall, e.g. the spawning places of *Anopheles gambiae*—the malaria vector—are located on backwater perimeter, whose length is equal to 0 in absence of rain (stable dry season), tends to infinity when backwater is progressively fulfilled by water (fractal transient phase during the season transition) and diminishes until $2\pi R$, where R is the radius of the final backwater mare (stable rainy season). During the susceptible host and infective *Anopheles* spread, the maximum of contagion is observed on the common zones of least diffusion of both hosts and vectors, which can be asymptotically confounded: as for the morphogens interaction in morphogenesis, the common zero-diffusion domain allows a maximum of contagious contacts between interacting species (Abbas et al. 2009).

During the stable rainy season, taking into account the diffusion of all vector subpopulations A_s, A_g and A_i (*Anopheles* susceptible, infected/non infective and infective) until the human subpopulations S, G, I and R (susceptible, infective, infected/non infective and recovered), it is possible to simulate the model and compare its numerical results to the data recorded on the ground, showing a good fit. In order to improve this fit, contagion parameters are chosen depending on space, e.g. maximum in zones where diffusion of infective vectors and hosts (whose concentration is respectively A_i and G) is minimum and in zones where concentration of susceptibles (A_s and S) is maximum ensuring locally a large coexistence time, hence a high contagion rate between large interacting subpopulations (Dutertre 1976).

In case of isotropic diffusion, the zero Laplacian (or zero curvature or maximal gradient) lines of the concentration surfaces of the concerned populations become, if they intersect, a contagion frontier, where hosts, vectors and infectious agents interact. These lines correspond to regions where the mean Gaussian curvatures on surfaces of concentration S and A_i, defined respectively by $\partial^2 S/\partial x^2 \partial^2 S/\partial y^2 - (\partial^2 S/\partial x \partial y)^2$ and $\partial^2 A_i/\partial x^2 \partial^2 A_i/\partial y^2 - (\partial^2 A_i/\partial x \partial y)^2$, vanish. Figure 3 shows the possibility of

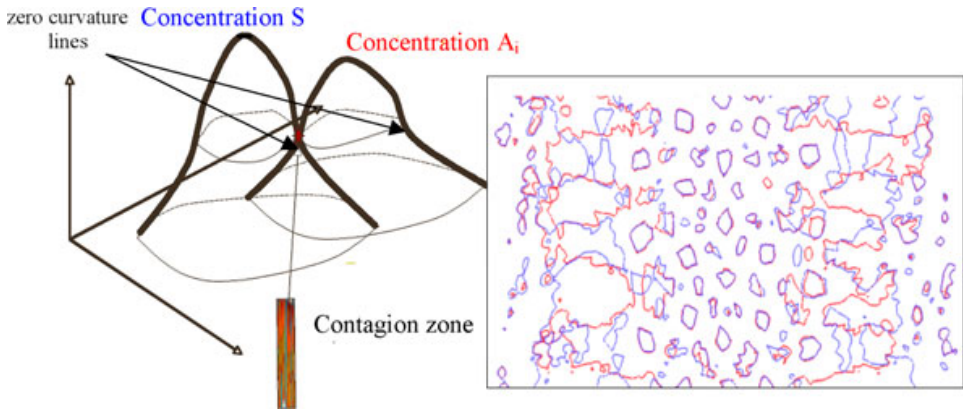

Fig. 3 Representation of the co-evolution of the zero-diffusion domains for interacting species S (*blue*) and A_i (*red*) in case of isotropic diffusion (*left*). Asymptotic co-existence of S and A_i on their common least diffusion domain (*right*)

such an intersection on only one tangency point or two intersection points (left) and on whole zero-diffusion curves asymptotically confounded (right) for a convenient value of the ratio between the diffusion coefficients D_S/D_{Ai} (Abbas et al. 2009).

5 Biological Age Definition

The discrete Usher matrix Eq. 6 can be replaced by its continuous equivalent modelling the population growth, e.g. a von Foerster-like partial differential equations, where σ_S denotes the biological age shift of an individual susceptible with respect to its chronological age t:

$$\sigma_S S_x(a,t) + S_t(a,t) = -\mu_S S(a,t), \tag{12}$$

where $S(a, t)$ is the number of susceptibles in biological age a at time t.

If the dependence on the biological age authorizes the ageing acceleration γ_S of an individual with respect to its chronological age t, the generalized von Foerster equation can be used (Demongeot 2009):

$$\sigma_S S_x(a,t) + \Box S + S_t(a,t) = -\mu_S S(a,t), \tag{13}$$

where the demographic d'Alembertian operator is equal to $\Box S = \gamma_S \partial^2 S/\partial a^2 - \Delta N$ and where μ_S is the natural mortality coefficient of the susceptibles (Demetrius 1979; Demongeot 1983; Brouns and Denuit 2001).

The same type of equation can be used for all host and vector population dynamics. The values of parameters like σ_S, γ_S and μ_S can depend both on space, biological age and time.

6 Introduction of Saturation Kinetics and Genetic Drifts

As noticed in (Horie et al. 2010), the viral genome is easily mutating and transferring new genes to both hosts and vectors, these latter being often also hosts and rarely

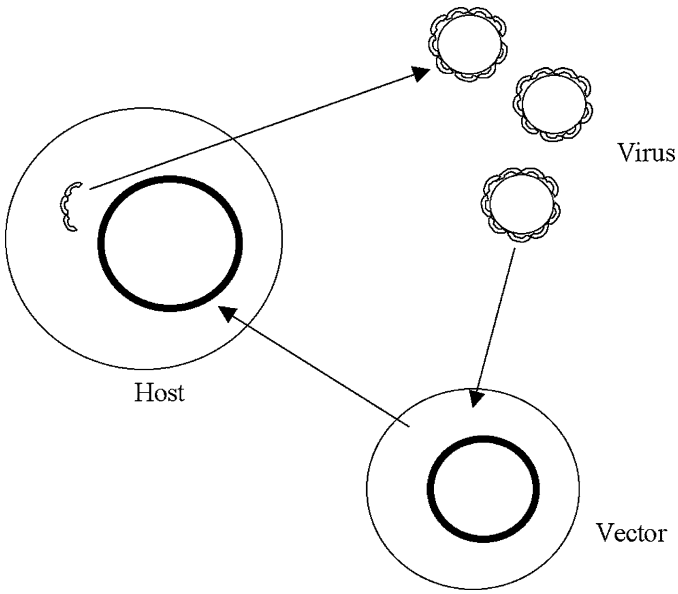

Fig. 4 The triple wins game in which hosts and vectors use the viral genome for making evolve their own genomes, and the viruses survive thanks to these latter, which code for their proteins

neutral healthy carriers. The vast majority of these new genes apparently do nothing, but some still produce working proteins or contribute to code for small regulatory RNAs (siRNAs or miRNAs) or for RNA-binding oligo-peptides, important traduction factors. It is yet impossible to know what these RNAs, peptides or proteins exactly do. But our ancestors have domesticated their viral interlopers to act as partners of our cells (Fig. 4). In the example discovered by (Horie et al. 2010), bornaviruses have clearly taken part to the evolution of mammals.

Taking into account in the models of viral epidemics these genetic transfer could allow to explain the apparition of resistances both in hosts and vectors diminishing their ability to build viral proteins, and also on the viral side, could render explicit certain strategies for escaping the host immunologic defences (Demongeot et al. 2009; Thuderoz et al. 2010). A way to incorporate this triple win game (wins for hosts, vectors and also infectious agents which have survived and coexist together during the evolution) consists in rendering dependent the contagion, fecundity, longevity and death parameters of both hosts and vectors on the level of contact represented by the term βSA_i. This dependence is supposed to decrease β, σ, γ and μ, and at the same time increase f: indeed, the largest is the contact number, the most adapted in terms of low susceptibility, high fecundity and longevity are the population of hosts and vectors offering to the infectious agent numerous targets to survive, and to hosts and vectors a way to evolve rapidly in order to increase their adaptive power. The decreasing functions could be linear between two thresholds, the upper corresponding to the situation of a new infectious agent whose virulence is maximal, and the lower to endemics resulting from a long cohabitation between the infectious disease actors. The advantage for vectors would be for example clear, if the host disease causes also a disease in the vector, because evolved vectors with resistance would be healthier and would have an adaptive advantage. The strategy of infectious agents would be then to evolve around the vector's and host's defences, circumventing and overcoming them (Baum et al. 2004). The observation in model simulations of a periodic time evolution of the parameter values with the possibility to randomly reset them at their upper threshold values (representing the

mutation of an ancient virus or the occurrence of a new one) could render the model more realistic hence more adapted to simulated scenarios for testing public health policies and anticipating real epidemics or pandemics.

7 Black Death

7.1 Introduction

Plague was considered as endemic in the steppes of Southern-Russia where Mongols originated (Zhang et al. 2008). Born in the Caspian sea area (probably triggered by contacts between Mongolian and Genoa sailors and warriors in wars around 1346), the European epidemic wave went through the mean of Mediterranean routes (Fig. 5). It reached ports like Marseilles in France and Genoa in Italy at the end of the year 1347. During 5 years it was spread widely in Europe from these two large commercial cities and come back to the Caspian reservoir. A simple Susceptibles-Infectives model with Diffusion (SID) explains the essential of the observed front wave dynamics during years between 1348 and 1350. The model uses only 3 coefficients: (1) a local viscosity proportional to the altitude, (2) a

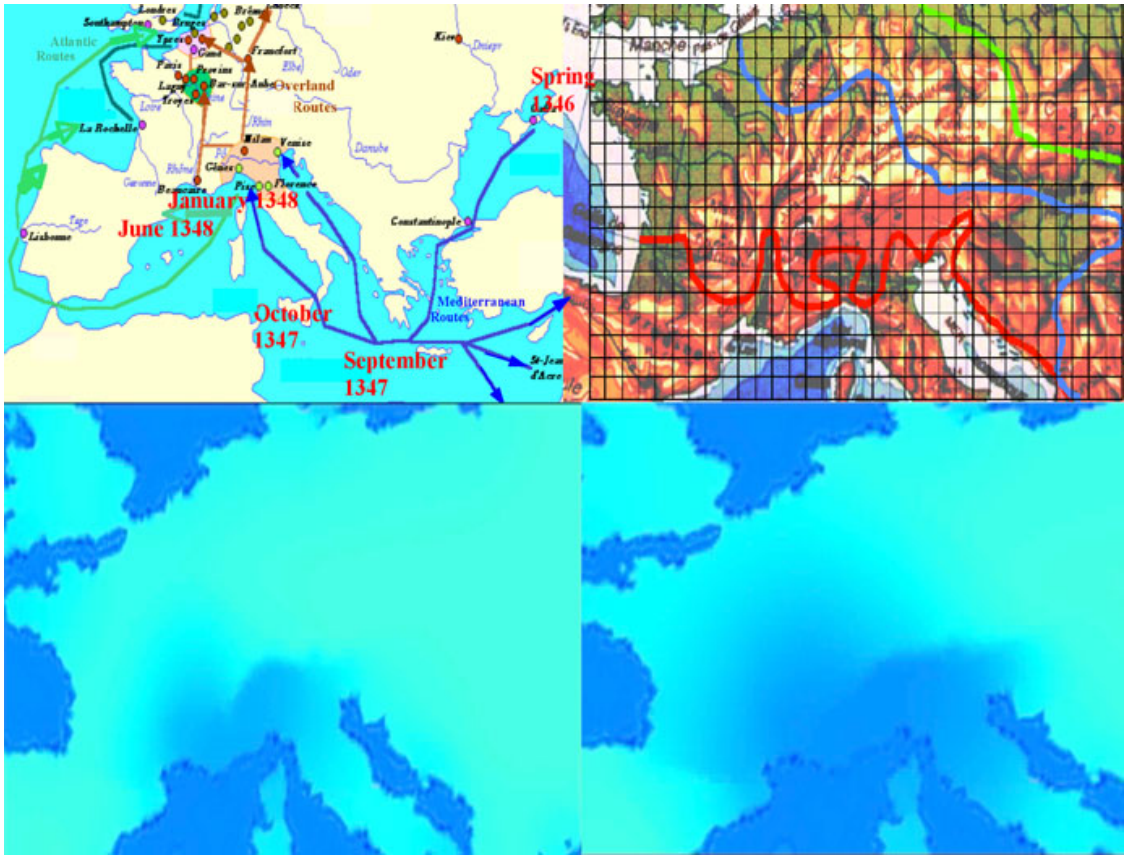

Fig. 5 *Top left* The spread of bubonic plague following see and overland routes (after <http://www.cosmovisions.com/ChronoPestesMA02.htm>). *Top right* Observed wave fronts after 1 (*red*), 2 (*blue*) and 3 (*green*) years of spread from the 2 initial entry ports Marseilles and Genoa (after Mocellin-Spicuzza 2002); the black grid corresponds to the collected altitudes. *Bottom* Simulation of the wave front after 3 (*left*) and 6 (*right*) months from the 2 initial entry ports Marseilles and Genoa

contagion parameter and (3) a death/recovering parameter (representing the future of infecteds as dead or immunized after being cured of the plague).

7.2 The Raw Data

Data are coming from numerous different sources, like parish, bishop, monastery and hospital registers, abbey cartularies, town council registers, e.g. *riformagioni* in Italy (Carpentier 1993), cemeteries,… For example, a part of data comes from a monastic order, the Hospitaller Order of St Anthony founded at La Motte (presently Saint Antoine) in the Dauphiné (France) in 1095 near Grenoble by Gaston du Dauphiné, whose son was struck by a fungal disease, known in the Middle Ages as Saint Anthony's fire (ergotism), caused by a transformation of the grain (often rye) into enlarged, hard, brown to black spur-like structures that constitute the source of the drug ergot in flour and causes convulsions often leading to death. The members of this Order were specialised in curing patients suffering from this disease. The Order was approved by Pope Urban II during the Council of Clermont in 1095. Later in 1218, Pope Honorius III permitted the brothers to take the vows of obedience, poverty and chastity. In the thirteenth century the Order spread over the whole of Western Europe with about 370 hospitals in the fourteenth century, able to treat about 4,000 patients. This organization permitted to the order to receive about 1,500 patients suffering of the plague and since 1339 has been in relationship with the University of Grenoble under the Dauphin Humbert.

The origine of the Black Death epidemics is uncertain (Wheelis 2002). Wars between Mongols and Chinese contributed to its dissemination in Asia. In 1334, in the North-Eastern Chinese province of Hopei, the plague was particularly virulent and killed about 90% of the population—some 5 million people. Then it went in Europe from east, striking Caucasia and Crimea (Wheelis 2002). In 1346, Tatars attacked the port of Caffa, presently in Ukraine but belonging at this time to Genoa. After an agreement between Genoa and Tatars, the conflict ceased and ships from Caffa transmitted the disease in each ports at which they stop. Hence in 1347, the Black Death arrived first in Constantinople, then in the Mediterranean trade cities: Messine in Sicily, and after Genoa (where commercial boats were sent back for a time) and Marseilles (where boats have been accepted for commercial reasons) at start of the year 1348.

The diffusion of the plague is probably due to rat infestations and abundant fleas in trade ships, transmitting plague to city rat populations (Wheelis 2002). From bubonic plague, the outbreak continuation appears to have been mainly due to the direct pneumonic transmission. From Marseilles, plague devastated Provence reaching Avignon—100 km far from Marseilles—in 1 month, respecting the estimation of the front speed given in (Murray 2002) and went through the Rhône valley until Paris. Some says the maximal velocity was 75 km a day, i.e. 87 cm/s, which is notably larger than the estimation of 5 cm/s made in (Murray 2002). This maximal velocity probably occurred only in zones with diffusion maximum, i.e. with viscosity minimum, like the Rhône Valley (maximal human density and commercial transactions). During the next 3 years of the epidemics, it spread northwards, reaching Norway and crossing to England and from there to Scotland,

Ireland, Iceland and Greenland. Mortality of the pandemic was terrible: at least 25 million people, that is 25–75% of the European population (Russell 1948) are estimated to have died, e.g. at Givry in Burgundy for about 1,500 inhabitants, the parish register shows 649 funerals in 1348, whose 630 from June to September. The parish having normally only 40 funerals the year, the specific mortality rate due to plague was equal to $(649 - 40)/1{,}500 = 40.6\%$. Another example is a sample of 235 deaths from the bishop's registers of Coventry and Lichfield, the only English register to list both date of death and date of institution, showing that the Black Death swept through very rapidly to local areas (Wood 2003).

The influence of climate on the outbreak is controversial. It is likely that a harsh climate, combined with the poverty, population and war (the Hundred Years' War), has been an important risk factor (Zhang et al. 2008). Furthermore, emerging from the dark ages, overland and see trade routes have been developed and the population density increased in the cities, favouring epidemics. It is now believed that bubonic plague (*Yersinia pestis*) is the infectious agent of the Black Death (Raoult et al. 2000). Sometime in the past, *Yersinia pestis* lost a set of genes expressed as adhesins, binding the bacteria to intestinal crypts (Orent 2001, 2004). Now, by suppressing signals between immune cells, plague spreads through the lymphatic system, invading organs such as spleen, lungs, and especially the liver. Bubonic plague is transmitted indirectly (mainly by flies), has an incubation period of 2–6 days and a mortality rate between 50 and 90% (if untreated). Pulmonary plague can be secondary to a bubonic plague or primary after direct contamination. Highly contagious, the primary pulmonary plague occurs from an aerial contage (direct by respiratory droplets) and if no treated the disease is fatal in most cases. Its incubation period is between 2 and 4 days, with $R0$ estimated varying between 0.8 and 3, with mean 1.3 (Gani and Leach 2004).

Knowledge about the demographic dynamics needs data about the population growth in middle-age cities (Renouard 1948; Russell 1972; Mocellin and Experton 1992; Brossollet and Mollaret 1994; Horrox 1994; Mischlewski 1995; Drancourt et al. 1998; Eckert 2000; Cantor 2001; Wood 2003; Mocellin-Spicuzza 2002; Cohn 2002; Scott and Duncan 2004; Benedictow 2004; Christakos et al. 2005; Kelly 2005; Barry and Gualde 2006) like Florence in Italy, whose population passed from about 100,000 inhabitants in 1338—90,000 in 1336 for (Villani 2001)—to 50,000 in 1351. Parallelly, during this period of time, between 60 and 70% of Hamburg's and Bremen's population died and in Provence, Dauphiné or Normandy, historians observed a decrease of 60% of fiscal hearths in French cities of these regions (cf. http://www.answers.com/topic/ and http://www.io.com/~sjohn/demog.htm). In some regions, two-thirds of the population were annihilated. About half of Perpignan's population died in several months (only two of the eight physicians survived the plague). England lost 70% of its population, which passed from 7 million to 2 million in 1400. Big European cities ranged from 12,000 to 100,000 people, with some exceptional cities exceeding this scale. Some historical examples before Black Death included London (25,000–40,000), Paris (50,000–80,000), Genoa (75,000–100,000) and Venice (100,000). Moscow in the fifteenth century had only a population in excess of 200,000! No complete population censuses were taken until the eighteenth century, thus estimates of population levels are notoriously unreliable. Estimated levels vary as a number of "multiplier" factors which often have to

be taken into account: estimated population density, ages of marriage, and perhaps most importantly the number of people denoted by a "hearth" in medieval tax surveys that do provide hard numbers.

7.3 The Model

The Fisher equation (Fisher 1937; Murray 2002) has been firstly used for representing the evolution of the host and vector sub-populations during the spread of the Black Death:

$$\frac{\partial S}{\partial t} = \lambda S(1 - S/S_0) + \kappa \partial^2 S/\partial x^2, \tag{14}$$

where λ in the logistic term is the growth rate at the homogeneous limit (S independent of the space variable x), S_0 is a saturation size, and κ is the diffusion coefficient (the inverse of the viscosity). Equation 14 admits propagating wave solutions of the form $S(x, t) = S(x - v_{front}t)$, with $v_{front} \approx 2(\kappa\lambda)^{1/2}$ as speed of the front (Murray 2002). The case of a heterogeneous medium is treated in (Mendez et al. 2003). Murray quoted a diffusion coefficient κ of about 10^3 m^2/s and a reaction (growth) rate of 15 year^{-1}, corresponding to $\lambda \sim 5\ 10^{-7}$ s^{-1} and giving an estimation for v_{front} of about 5 cm/s, i.e. about 1,500 km/year (Brandenburg and Multamaki 2004).

The model used in this paper for modelling the Black Death spread is a SIRD model as in the Bankoumana study (Gaudart et al. 2007, 2009, 2010), but without vector terms and has for its reaction term the form of a Lotka-Volterra Ordinary Differential Equation (ODE) of dimension 3, plus a diffusion term:

$$\frac{dS}{dt} = \varepsilon\Delta S - \beta SI, \quad \frac{dI}{dt} = \varepsilon\Delta I + \beta SI - \gamma R, \quad \frac{dR}{dt} = \varepsilon\Delta R + \gamma R, \tag{15}$$

where βSI term comes from the "law of mass action", assuming homogeneous mixing between susceptibles and infecteds, β is the rate of transition from susceptible to infected state, calculated per infected and per susceptible, γ is the rate of transition from infected to post-infected state (e.g. death or immunity) per infected person and ε is the diffusion coefficient. By taking the viscosity (inverse of ε) proportional to the altitude, the simulated front waves are more similar to the observed ones (Fig. 5) than in the previous simulations (Murray 2002). The initial population size of susceptibles in the main middle age cities has been fixed following the demographic data. The results of simulations (Fig. 5 bottom) are in agreement with the data observed in the 370 hospitals of the order of St Anthony (Fig. 5 top right). Improvements could come from considering multiple entrance points (ports like Barcelona reached in June 1348 or La Rochelle, Rouen and Dover reached later in 1348), and taking into account all the commercial sea (Mediterranean and Atlantic) and overland routes (Fig. 5 top left) as well as the demography (fecundity and natural mortality, as well as more sophisticated notions as demographic potential and Hamitonian demographic energies (Maupertuis 1745, reed. 1965; Thom 1972; Demongeot and Demetrius 1989; Porte 1994; Demongeot et al. 2007a, b; Forest et al. 2007; Glade et al. 2007)).

The present endemic state (Fig. 6) could be explained by a new model taking into account the air routes (La peste humaine 1997; WHO 1999). Plague is still important

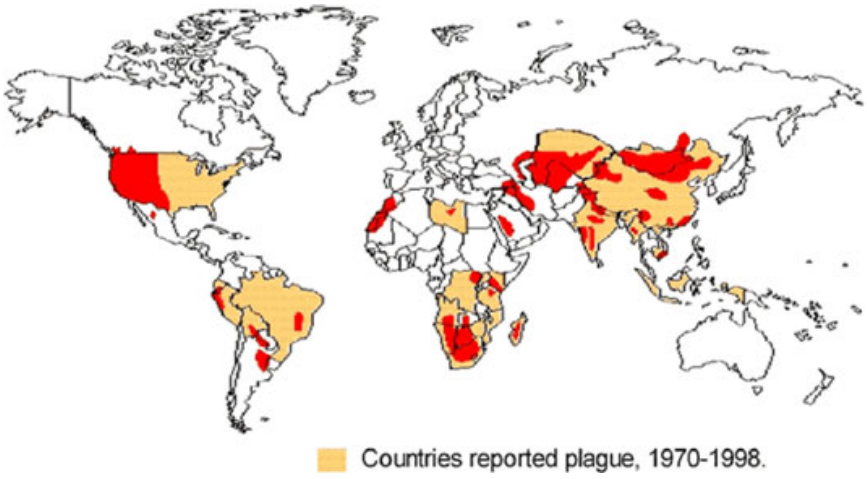

Fig. 6 World distribution of plague in 1998 (after WHO 1999)

because it could be considered as a re-emerging disease (Stenseth et al. 2008): *Yersinia pestis* still causes several thousand human cases per years and about hundred human deaths are reported each year. Plague is present in all continents, as human and enzootic disease, particularly in Africa, North and South America, and Asia (Prentice and Rahalison 2007). Democratic Republic of the Congo and Madagascar are particular places, accounting most of the reported cases (Neerinckx et al. 2008). Most of the present cases correspond to bubonic plague, but outbreaks of pneumonic plague still occur. Environmental, geographical and social characteristics are particularly favourable for a broad diffusion of plague in Africa (Neerinckx et al. 2008), in spite of the focal nature of the transmission. *Yersinia pestis* is also an attractive agent for bioterrorism (Wheelis 2002; Prentice and Rahalison 2007; Zhang et al. 2008). Furthermore, climate change might modify the dynamics of plague transmission and cause outbreaks in endemic regions but also in non-endemic regions (Raoult et al. 2000; Stenseth et al. 2008). Crisis-management approach is considered as insufficient (Orent 2001, 2004) and prevention action would be more effective. An efficient prediction from simulations of a realistic model taking into account the new aerial routes with minimal viscosity (Khan et al. 2009) could serve this cause.

8 The Malaria in Mali

8.1 Introduction

The malaria is a parasitic infectious disease whose agent belongs to the genus *Plasmodium* (essentially *P. falciparum*). Malaria is carried by the mosquitos of the genus *Anopheles* and the vector in Mali is *Anopheles funestus* or *Anopheles gambiae* (Depinay et al. 2004; Huang et al. 2006; Gaudart et al. 2009). Symptoms of malaria include fever, headache and vomiting, and usually appear between 10 and 15 days after the mosquito bite. Untreated, malaria becomes life-threatening by disrupting the blood supply to vital organs. In southwest of Mali in particular in the region near the river Niger each rainy season triggers annual malaria epidemic. The WHO's

statistics say malaria accounts for 17% of child deaths in Mali. One in five Malian children die before their fifth birthday. Of the one to three million people worldwide who die of malaria every year, 90% live in sub-Saharan Africa. Malaria kills an African child every 30 s, according to WHO. Of those, several hundred thousand live in the Sahel region of West Africa, which encompasses Mali, Mauritania, Niger, Burkina Faso, Chad and parts of Senegal, Togo, Benin and Nigeria. The Bankoumana village is a locality of Sudanese savannah area in Mali in which the disease has been carefully studied and recorded since 15 years. At each evaluation on the ground (each 2 months during the rainy season and each 3 months during the dry one) a blood sample is collected on each child of the village and the parasitemia is studied for *Plasmodia falciparum*, *malariae* and *ovale*, as well as the gametocytemia (for *P. falciparum*), with Giemsa technique (Doumbo 2005).

8.2 The Model

The model has been drawn in order to take into account the known mechanism of the disease and to qualitatively fit the empirical observations. The equations are given in Fig. 7, without age classes for host nor for vector, but with diffusion for vector (supposed to be much larger than the host diffusion). The contagion parameters $\alpha\beta$ and $\alpha\zeta$ can be chosen depending on space, in particular α, the mean bite number per mosquito and per night. During the stable rainy season, taking into account the diffusion of all vector subpopulations A_s, A_g and A_i (*Anopheles* susceptible, infected/non infective and infective) until the human subpopulations S, G, I and R (susceptible, infective, infected/non infective and recovered), it is possible to simulate the model and compare its numerical results to the data recorded on the ground, showing a good fit. For improving the fit, contagion parameters have been chosen depending on space, e.g. fixed at a value maximum in

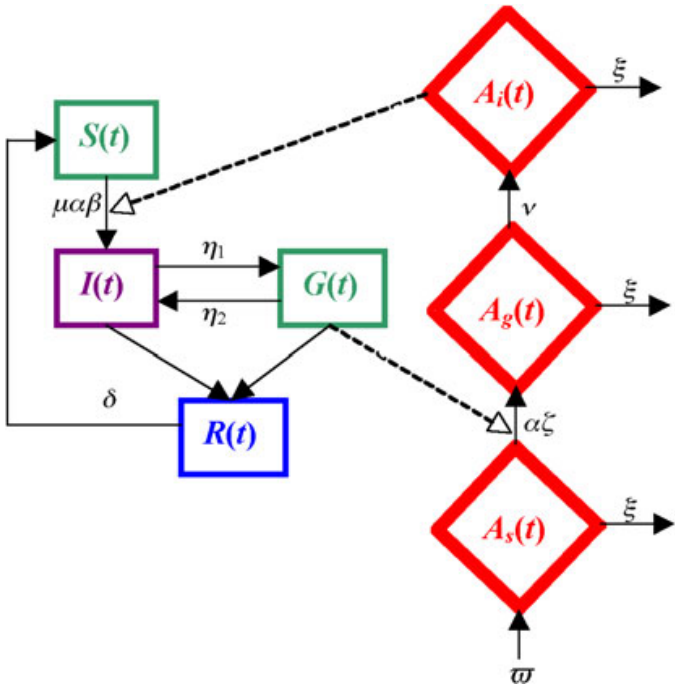

Fig. 7 Interaction graph (*top*), and SIGR Diffusion (SIGRD) Eq. 16 both for hosts and for vectors (*bottom*) for the Bankoumana model

zones where diffusion of infective vectors and hosts (A_i and G) is minimum, and in zones where the concentration of susceptibles (A_s and S) is maximum.

$$\begin{aligned}
\frac{dS}{dt} &= -\mu\alpha\beta SA_i + \delta R \\
\frac{dI}{dt} &= \mu\alpha\beta SA_i - (\eta_1 + \gamma)I + \eta_2 G \\
\frac{dG}{dt} &= \eta_1 I - (\eta_2 + \gamma)G \\
\frac{dR}{dt} &= \gamma(I + G) - \delta R \\
\frac{\partial A_s}{\partial t} &= D_s \Delta A_s + \varpi - \alpha\varsigma G A_s - \xi A_s \\
\frac{\partial A_g}{\partial t} &= D_g \Delta A_g + \alpha\varsigma G A_s - (\xi + v)A_g \\
\frac{\partial A_i}{\partial t} &= D_i \Delta A_i - \xi A_i + v A_g
\end{aligned} \tag{16}$$

The variables of the Bankoumana model are:

$S(t)$: size of the sub-population of Susceptible hosts
$I(t)$: size of the sub-population of Infected not Infective hosts (positive parasitemia and negative gametocytemia)
$G(t)$: size of the sub-population of infective hosts by Gametocytes hosts (positive gametocytemia)
$R(t)$: size of the sub-population of Resistant hosts, i.e. treated and resistant to the disease, or immunized, died or deplaced
$As(t)$: size of the sub-population of Susceptible *Anopheles*
$Ag(t)$: size of the sub-population of infected (but not infective) *Anopheles* by Gametocytes,
$Ai(t)$: size of the sub-population of Infective *Anopheles*
$N(t)$: total size of hosts
$M(t)$: total size of *Anopheles*

The parameters of the Bankoumana model are:

δ: rate of immunization loss in host ($1/\delta$ is the mean duration of the resistance)
η_1: rate of gametocytes occurrence in host ($1/\eta_1$ is the mean duration of the time interval between the primo-infection and the first appearance of gametocytes in an infected individual)
η_2: rate of gametocytes loss in host
γ: rate of resistance occurrence
μ: Anophelian density, i.e. *Anopheles* number per host
α: mosquito bite rate per mosquito and per night ($\mu\alpha$ is called the vector agressivity)

In the model, a Susceptible can become Plasmodic Infected (non Infective). A Plasmodic Infected can shift to the Gametocytic state, or recover and acquire an immunization, or recover without immunization, i.e. become a new susceptible. The

immunized state can also naturally disappear (e.g. due to an intercurrent disease paralysing the immune system). The introduction of the space in the model could be done by using stochastic spatial Markovian or renewal models (Demongeot and Fricot 1986) or deterministic Partial Differential Equations (PDE). Such models are of SIGRD type (de Magny et al. 2005).

The Bankoumana model (Fig. 7 bottom, Eq. 16) is a double SIGRD model (Gaudart et al. 2007, 2009) whose interaction graph (Fig. 7 top) corresponds to PDE Eq. 16 with spatial initial conditions essentially determined by the spawning zones in backwater places (Fig. 6 bottom). These zones are depending on the rainfall hence have a seasonal occurrence (Balenghien et al. 2006; Bicout et al. 2002; Bicout and Sabatier 2004; Ndiaye et al. 2006; Porphyre et al. 2004): the spawning places of *Anopheles gambiae*—one of the malaria vectors—are located on the backwater perimeter, whose length is equal to 0 in absence of rain (stable dry season), tends to infinity when backwater holes—puddles or ponds—are progressively fulfilled by water (fractal transient phase during the season transition) and diminishes until $2\pi R$, where R is the radius of the final backwater hole (stable rainy season). During the stable rainy season, taking into account the diffusion of all vector subpopulations A_s, A_g and A_i (*Anopheles* susceptible, infected/non infective and infective) until the human subpopulations S, G, I and R (susceptible, infective, infected/non infective and recovered) supposed to be fixed, we can simulate and compare the numerical results to the data recorded on the ground, showing a good fit (Fig. 8). For

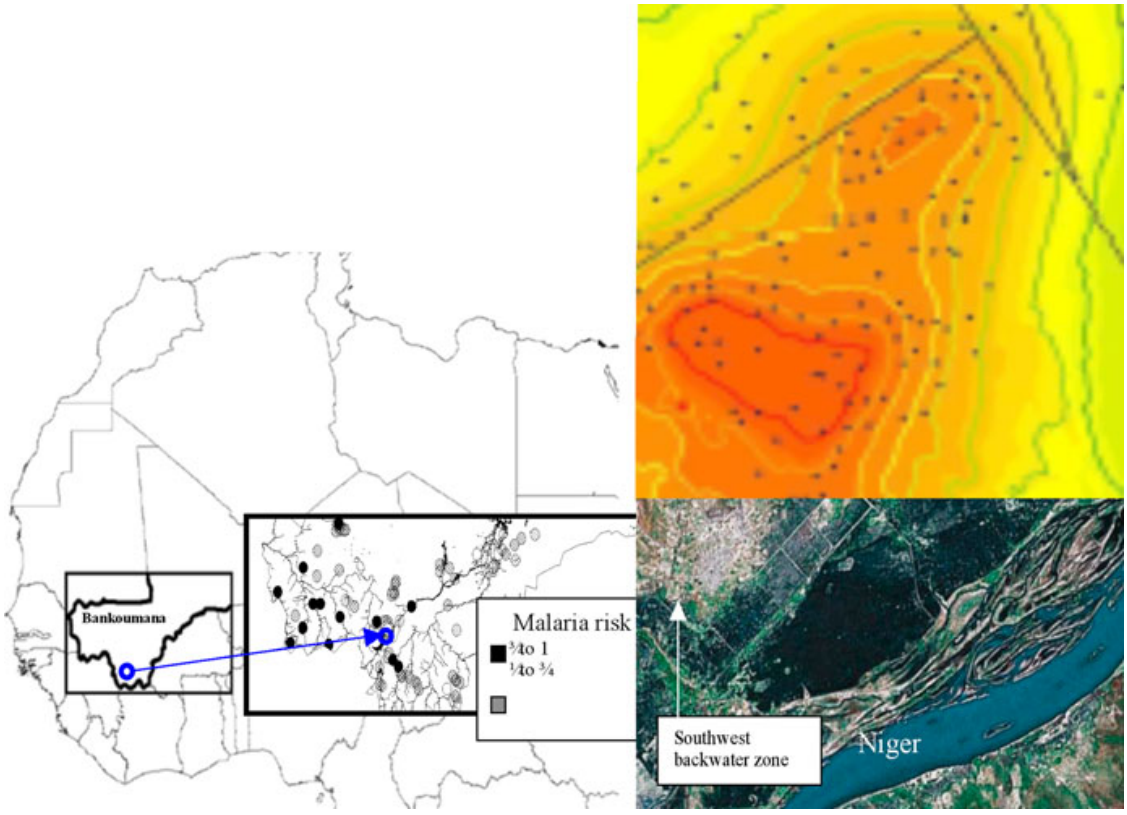

Fig. 8 Results of the SGIRD simulated (*top right*) and real data (*middle right*) showing a good fit along a gradient parallel to Niger river from the southwest backwater zone (*bottom*) to the village of Bankoumana (Mali)

improving this fit, contagion parameters β and ζ can be chosen depending on space, e.g. maximum in zones, which constitute overlaps between domains where diffusion of infective vectors and hosts (A_i and G) is minimum and domains where concentration of susceptible (A_s and S) is maximum, ensuring locally a large coexistence time, hence a high contagion rate between these interacting subpopulations (Abbas et al. 2009).

If we simplify the malaria model (16), by considering only the population of infected and contagious vectors, we can introduce in the equations a delay θ in order to take into account the long incubation period both in host and vector, due in particular to host and vector migrations and climatic changes (which explains in part that malaria is reappearing in south of Europe). In this new model, the variables are denoted as follows:

$S(t)$ represents the size of the susceptible host population,
$I(t)$ represents the size of the infected but not contagious host population,
$G(t)$ represents the size of the infected and contagious host population,
$R(t)$ represents the size of the resistant host population,
$A_i(t)$ represents the size of the infected and contagious vector population,
$VI(t)$ represents the Normalized Difference Vegetation Index (NDVI), i.e. a simple numerical indicator coming from remote sensing measurements assessing whether an observed zone contains live green vegetation or not.

The parameters of the new model are defined as follows:

Parameters	Definition
α	Mosquito bite rate per mosquito and per night ($\mu\alpha$ is called the vector agressivity)
β	Probability for a susceptible human of becoming infected after a single bite
γ	Rate of resistance occurrence
δ	Rate of immunization loss in host ($1/\delta$ is the mean duration of the resistance)
ς	Probability for an susceptible *Anopheles* of becoming infected after a single bite on an infected human
η_1	Rate of gametocytes occurrence in host ($1/\eta_1$ is the mean duration of the time interval between the primo-infection and the first appearance of gametocytes in an infected individual)
η_2	Rate of gametocytes loss in host
θ	Latency period for the normalized vegetation index
μ	Anophelian density, i.e. *Anopheles* number per host
υ	Average duration of the gonotrophic cycle
ξ	Mortality rate of the susceptible *Anopheles*
τ	NDVI lowest threshold value conditioning the *Anopheles* behavior

The transition from susceptible to infected state depends on host (resp. vector) population size, but also on climatic factors represented by the variable $i(t)$ (resp. $i_m(t)$) in equations (T_0):

$$\begin{cases} \frac{dS(t)}{dt} = -i(t)S(t) + \delta R(t) \\ \frac{dI(t)}{dt} = i(t)S(t) - (\eta_1 + \gamma)I(t) + \eta_2 G(t) \\ \frac{dG(t)}{dt} = \eta_1 I(t) - (\eta_2 + \gamma)G(t) \\ \frac{dR(t)}{dt} = \gamma[I(t) + G(t)] - \delta R(t) \\ \frac{dA_i(t)}{dt} = i_m(t)\left[\exp\left\{\frac{-\xi\upsilon}{1+\chi_{\{VI(t-\theta)\geq\tau\}}VI(t-\theta)}\right\} - A_i(t)\right] - \frac{\xi}{1+\chi_{\{VI(t-\theta)\geq\tau\}}VI(t-\theta)}A_i(t) \end{cases} \tag{17}$$

$$\text{with : } \begin{cases} i(t) = \mu\alpha\beta\chi_{\{VI(t-\theta)\geq\tau\}}VI(t-\theta)A_i(t) \\ i_m(t) = \alpha\varsigma[\chi_{\{VI(t-\theta)\geq\tau\}}VI(t-\theta)]G(t) \end{cases}$$

By denoting $\begin{cases} a = \mu\alpha\beta[\chi_{\{VI(t-\theta)\geq\tau\}}VI(t-\theta)] \\ b = \alpha\varsigma[\chi_{\{VI(t-\theta)\geq\tau\}}VI(t-\theta)] \end{cases}$ and $\Delta = \frac{-\xi}{1+\chi_{\{VI(t-\theta)\geq\tau\}}VI(t-\theta)}$, the previous equations become the following system:

$$(T_1) = \begin{cases} \frac{dS(t)}{dt} = -aA_i(t)S(t) + \delta R(t) \\ \frac{dI(t)}{dt} = aA_i(t)S(t) - (\eta_1 + \gamma)I(t) + \eta_2 G(t) \\ \frac{dG(t)}{dt} = \eta_1 I(t) - (\eta_2 + \gamma)G(t) \\ \frac{dR(t)}{dt} = \gamma[I(t) + G(t)] - \delta R(t) \\ \frac{dA_i(t)}{dt} = bG(t)[\exp(\Delta\upsilon) - A_i(t)] + \Delta A_i(t) \end{cases} \tag{18}$$

The two stationary states of (T_1) are the healthy state $E_0 = (S_0, 0, 0, 0, 0)$ and the endemic state $E^* = (S^*, I^*, G^*, R^*, A_i^*)$, where: $S_0 = \frac{1}{R_0}$; $S^* = \frac{1}{R_0\left(1-\frac{A_i^*}{\exp\left(\frac{-\xi\upsilon}{1+\chi_{\{VI(t-\theta)\geq\tau\}}VI(t-\theta)}\right)}\right)}$, $I^* = \frac{\eta_2+\gamma}{\eta_1}G^*; G^* = \frac{\mu\alpha\beta[\chi_{\{VI(t-\theta)\geq\tau\}}VI(t-\theta)]}{\gamma\left[\frac{\eta_1+\eta_2+\gamma}{\eta_1}\right]}A_i^*S^*$ and $R^* = \frac{\gamma}{\delta}\left[\frac{\eta_1+\eta_2+\gamma}{\eta_1}\right]G^*$, with $R_0 = \frac{\mu\alpha^2\beta\zeta[\chi_{\{VI(t-\theta)\geq\tau\}}VI(t-\theta)]^2\exp\left(\frac{-\xi\upsilon}{1+\chi_{\{VI(t-\theta)\geq\tau\}}VI(t-\theta)}\right)}{\frac{\xi}{1+\chi_{\{VI(t-\theta)\geq\tau\}}VI(t-\theta)}\gamma\left[\frac{\eta_1+\eta_2+\gamma}{\eta_1}\right]}$

$VI(t-\theta)$ is supposed to be constant equal to τ and $\Delta = -\xi/(1+\tau)$, when t is sufficiently large. We can notice that: $S_0 > S^*$. We will now study the stability of the first steady state E_0 by linearizing (T_1) and doing the change of variables: $x_1(t) = S(t) - S_0(t)$; $x_2(t) = I(t)$; $x_3(t) = G(t)$; $x_4(t) = R(t)$ and $x_5(t) = A_i(t)$, we get the system (T_2):

$$dx/dt = \begin{pmatrix} \dot{x_1} \\ \dot{x_2} \\ \dot{x_3} \\ \dot{x_4} \\ \dot{x_5} \end{pmatrix} = \begin{pmatrix} 0 & 0 & 0 & \delta & -aS_0 \\ 0 & -(\eta_1+\gamma) & \eta_2 & 0 & aS_0 \\ 0 & \eta_1 & -(\eta_2+\gamma) & 0 & 0 \\ 0 & \gamma & \gamma & -\delta & 0 \\ 0 & 0 & b\exp(\Delta\upsilon) & 0 & -\Delta \end{pmatrix} \begin{pmatrix} x_1 \\ x_2 \\ x_3 \\ x_4 \\ x_5 \end{pmatrix} = B_1(x) \tag{19}$$

The characteristic polynomial of B_1 is given by:

$$\det(B_1 - \lambda I) = \begin{vmatrix} -\lambda & 0 & 0 & \delta & -aS_0 \\ 0 & -[\lambda + (\eta_1 + \gamma)] & \eta_2 & 0 & aS_0 \\ 0 & \eta_1 & -[\lambda + (\eta_2 + \gamma)] & 0 & 0 \\ 0 & \gamma & \gamma & -(\lambda + \delta) & 0 \\ 0 & 0 & b\exp(\Delta\upsilon) & 0 & -(\lambda - \Delta) \end{vmatrix}$$

$$P_{B_1}(\lambda) = \lambda(\lambda + \delta)\big\{-[\lambda + (\eta_1 + \gamma)][\lambda + (\eta_2 + \gamma)](\lambda - \Delta) + \eta_1\eta_2(\lambda - \Delta) + \eta_1 abS_0 \exp(\Delta\upsilon)\big\}$$

Hence: $P_{B_1} = -\lambda^5 - A\lambda^4 - (B + C)\lambda^3 - (\delta B + D)\lambda^2 - \frac{1}{\delta}D\lambda$,
where:

$A = \eta_1 + \eta_2 + 2\gamma - \Delta + \delta$

$B = \gamma(\eta_1 + \eta_2 + \gamma) - \Delta(\eta_1 + \eta_2 + 2\gamma)$

$C = \delta(\eta_1 + \eta_2 + 2\gamma - \Delta)$

$D = \gamma\Delta(\eta_1 + \eta_2 + 2\gamma) - \eta_1 abS_0 \exp(\Delta\upsilon)$

All coefficients of the characteristic polynomial being negative, the largest eigenvalue is 0 and the Hessian dominant eigenvalue is strictly positive, then E_0 is unstable.

For the second steady state E^*, after linearizing (T_1) and changing variables as $x_1(t) = S(t) - S^*$; $x_2(t) = I(t) - I^*$; $x_3(t) = G(t) - G^*$; $x_4(t) = R(t) - R^*$ and $x_5(t) = A_i(t) - A_i^*$, we get the equations (T_3):

$$\begin{aligned} dx/dt &= \begin{pmatrix} \dot{x_1} \\ \dot{x_2} \\ \dot{x_3} \\ \dot{x_4} \\ \dot{x_5} \end{pmatrix} \\ &= \begin{pmatrix} -aA_i^* & 0 & 0 & \delta & -aS^* \\ aA_i^* & -(\eta_1 + \gamma) & \eta_2 & 0 & aS^* \\ 0 & \eta_1 & -(\eta_2 + \gamma) & 0 & 0 \\ 0 & \gamma & \gamma & -\delta & 0 \\ 0 & 0 & b[\exp(\Delta\upsilon) - A_i^*] & 0 & -(bG^* - \Delta) \end{pmatrix} \begin{pmatrix} x_1 \\ x_2 \\ x_3 \\ x_4 \\ x_5 \end{pmatrix} \\ &= B_2 x \end{aligned} \tag{20}$$

The characteristic polynomial of B_2 is given by:

$$\begin{aligned} P_{B_2}(\lambda) &= \det(B_2 - \lambda I_5) \\ &= \det\begin{vmatrix} -(\lambda + aA_i^*) & 0 & 0 & \delta & -aS^* \\ aA_i^* & -[\lambda + (\eta_1 + \gamma)] & \eta_2 & 0 & aS^* \\ 0 & \eta_1 & -[\lambda + (\eta_2 + \gamma)] & 0 & 0 \\ 0 & \gamma & \gamma & -(\lambda + \delta) & 0 \\ 0 & 0 & b[\exp(\Delta\upsilon) - A_i^*] & 0 & -[\lambda + (bG^* - \Delta)] \end{vmatrix} \end{aligned}$$

$= K_1 + K_2$, where:

$$K_1 =$$

$$-(\lambda + aA_i^*)\begin{vmatrix} -[\lambda + (\eta_1 + \gamma)] & \eta_2 & 0 & -aS^* \\ \eta_1 & -[\lambda + (\eta_2 + \gamma)] & 0 & 0 \\ \gamma & \gamma & -(\lambda + \delta) & 0 \\ 0 & b[\exp(\Delta\upsilon) - A_i^*] & 0 & -[\lambda + (bG^* - \Delta)] \end{vmatrix}$$

$$K_2 = -aA_i^*\begin{vmatrix} 0 & 0 & \delta & -aS^* \\ \eta_1 & -[\lambda + (\eta_2 + \gamma)] & 0 & 0 \\ \gamma & \gamma & -(\lambda + \delta) & 0 \\ 0 & b[\exp(\Delta\upsilon) - A_i^*] & 0 & -[\lambda + (bG^* - \Delta)] \end{vmatrix}$$

After some calculations, we get:

$$K_1 = -D_0\lambda^5 - D_1\lambda^4 - D_2\lambda^3 - D_3\lambda^2 - D_4\lambda - D_5, \text{ where:}$$

$$\begin{aligned}
D_0 &= 1 \\
D_1 &= \eta_1 + \eta_2 + \gamma + bG^* - \Delta + aA_i^* + \delta \\
D_2 &= (\eta_1 + \eta_2 + \gamma)(bG^* - \Delta) + \gamma(\eta_1 + \eta_2 + \gamma + bG^* - \Delta) \\
&\quad + (aA_i^* + \delta)(\eta_1 + \eta_2 + 2\gamma + bG^* - \Delta) + aA_i^*\delta \\
D_3 &= \gamma(\eta_1 + \eta_2 + \gamma)(bG^* - \Delta) - \eta_1 abS^*[A_i^* - \exp(\Delta\upsilon)] \\
&\quad + (aA_i^* + \delta)[(\eta_1 + \eta_2 + \gamma)(bG^* - \Delta) + \gamma(\eta_1 + \eta_2 + \gamma + bG^* - \Delta)] \\
D_4 &= (\gamma aA_i^* + \gamma\delta + aA_i^*\delta)[(\eta_1 + \eta_2 + \gamma)(bG^* - \Delta) + \eta_1 abS^*(A_i^* - \exp(\Delta\upsilon))] \\
&\quad + aA_i^*\delta\gamma(\eta_1 + \eta_2 + \gamma + bG^* - \Delta) \\
D_5 &= aA_i^*\delta\gamma(\eta_1 + \eta_2 + \gamma)(bG^* - \Delta) + \eta_1 a^2 bA_i^*S^*\delta[A_i^* - \exp(\Delta\upsilon)]
\end{aligned}$$

and $K_2 = -T_0\lambda^2 - T_1\lambda - T_2$ with:

$$\begin{aligned}
T_0 &= aA_i^*\delta\gamma \\
T_1 &= aA_i^*\delta\gamma(\eta_1 + \eta_2 + \gamma + bG^* - \Delta) + \eta_1 a^2 bA_i^*S^*\delta[A_i^* - \exp(\Delta\upsilon)] \\
T_2 &= aA_i^*\delta\gamma(\eta_1 + \eta_2 + \gamma)(bG^* - \Delta) + \eta_1 a^2 bA_i^*S^*\delta[A_i^* - \exp(\Delta\upsilon)]
\end{aligned}$$

Then we have:

$$P_{B_2}(\lambda) = -D_0\lambda^5 - D_1\lambda^4 - D_2\lambda^3 - (D_3 + T_0)\lambda^2 - (D_4 + T_1)\lambda - (D_5 + T_2)$$

If $VI(t - \theta)$ is supposed to be constant equal to a large value τ, which corresponds to a saturated contagion from hosts $G(t)$ for a given number of vector *Anopheles*, then $\exp(\Delta v)$ is small and all the coefficients of the characteristic polynomial are strictly negative, which is the necessary condition for the application of the Routh-Hurwitz criterion; by building the Routh-Hurwitz matrix, all the elements of its first column are positive, which corresponds to the fact that E^* is locally stable.

9 Perspectives

The last improvements come from the Mac Donald SI model of malaria spread (Mac Donald 1957), another extension of the Ross model, which has the following interaction graph given in Fig. 9 with the equations:

$$\begin{aligned}
\frac{dS_1}{dt} &= -\beta_2 S_1 I_2/N_H + rI_1 \\
\frac{dI_1}{dt} &= \beta_2 S_1 I_2/N_H - rI_1 \\
\frac{dS_2}{dt} &= \varpi + fS_2 - \beta_1 S_2 I_1/N_V - \delta S_2 \\
\frac{dI_2}{dt} &= fI_2 + kE_2 - \delta I_2 \\
\frac{dE_2}{dt} &= fE_2 + \beta_1 S_2 I_1/N_V - kE_2 - \delta E_2
\end{aligned} \tag{21}$$

where f (resp. δ) is the fecundity (resp. death) rate of the vector population (susceptible, infected and infective vectors being supposed to have the same fecundity and mortality), β_1 (resp. β_2) is the host (resp. vector) contagion parameter, N_H (resp. N_V) is the host (resp. vector) population size, the ratio $m = N_V/N_H$ is the vector/host ratio, k (resp. r) is the vector (resp. host) speed of passage from the infected/not infective (resp. infected) state to the infective (resp. susceptible) state. If $f = \delta - \mu$ (the fecundity compensating partly the mortality), the value of $R0$, the mean number of secondary infected vectors for one infective host, is equal to:

$$R0 = \beta_1 \beta_2 k N_V/[N_H \mu r(k + \mu)] \tag{22}$$

If $R0 > 1$, the stationary state (0, 0, 0, 0, 0) is unstable and the endemic stable stationary state is reached after a transient epidemic wave for the values:

$$i_1^* = I_1^*/N_H,\ i_2^* = I_2^*/N_V,\ e_2^* = E_2^*/N_V,$$

with $i_1{}^* = (R0 - 1)/(R0 + \beta_1/\mu)$, $i_2{}^* = i_1{}^* \mu r/[m\beta_2(1 - i_1{}^*)]$, $e_2{}^* = i_1{}^*(\delta - f)r/[km\beta_2(1 - i_1{}^*)]$.

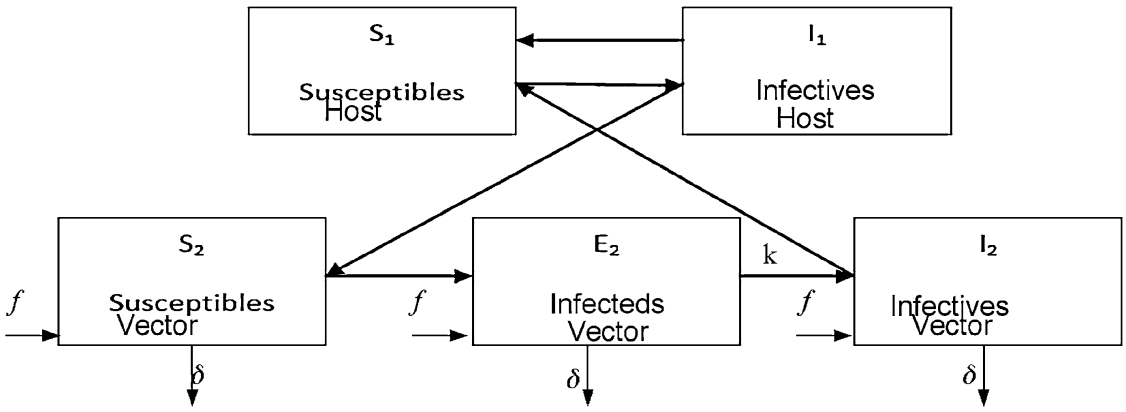

Fig. 9 Interaction graph of the Mac Donald model

If δ is small, then $k/(k+\delta) \approx e^{-\delta/k}$, where $1/k$ is the mean sojourn time in the compartment E_2 (sporogonic cycle duration) and $R0 = [\beta_1\beta_2 m/\delta r]\mathrm{e}^{-\delta/k}$.

Let us consider now the Cox model with proportional risk (Cooke and Morales-Napoles 2006) and suppose that the risk function would be given by $h(t, z) = \mathrm{e}^{\rho z}b(t)$, where ρ is a regression parameter and $b(\mathrm{t})$ the baseline risk function. Then, by denoting $u = \mathrm{e}^{\rho z}$, the survival function $S(t, u)$ (i.e. the probability to survive until the age t with a risk u) is given by:

$$S(t,u) = \exp\left[-\int_0^t h(s,z)ds\right] = B(t)^u, \tag{23}$$

where $B(t) = \exp\left[-\int_0^t b(s)\mathrm{d}s\right]$.

In the Mac Donald model, for calculating the survival function S_2 of the subpopulation I_2, it is possible to identify $z = \mathrm{Log}(\beta_1\beta_2 m/\delta r)$, $\rho = -k/\delta$, $t = 1/k$, $b(s) = \mathrm{cste} = \delta$, $B(1/k) = \mathrm{e}^{-\delta/k}$ and $R0 = [\beta_1\beta_2 m/\delta r]\mathrm{e}^{-\delta/k} = \exp[\mathrm{Log}(\beta_1\beta_2 m/\delta r)]\,\mathrm{e}^{-\delta/k} \approx S_2(1/k,(\beta_1\beta_2 m/\delta r)^{-k/\delta})$, if $\beta_1\beta_2 m/\delta r$ is close to 1. If there exist n age classes into the vector subpopulation E_2 whose sojourn times T_i ($i = 1, \ldots, n$) are independent random variables related to the survival functions S_i, we have:

$$P(T_i > t_i,\ i = 1,\ n \mid u) = \Pi_{i=1,n} S_i(t_i,u) = \Pi_{i=1,n} B_i(t_i)^u \tag{24}$$

If z is a random variable, then $u = e^{\rho z}$ is also a random variable and we define the mean survival function as $S(t) = \mathrm{E}_u[B(t)^u]$. If we consider now the Laplace transform defined by: $\mathrm{E}_u[\mathrm{e}^{-vu}] = \exp(-vp) = L(v)$, where p is a parameter depending on the probability distribution of u, we can write:

$$\begin{aligned} P(T_i > t_i, i = 1, n \mid u) &= [\exp(-\Sigma_{i=1,n}(-\mathrm{Log}[S_i(t_i)^{1/p}])^p = \Pi_{i=1,n} L_i(v) \\ &= C(S_1, \ldots, S_\mathrm{n}), \end{aligned} \tag{25}$$

where C is an Archimedean copula (Beaudoin and Lakhal-Chaieb 2008).

By introducing now a demographic dynamics and by using the Archimedean copula methodology, we can deal with a proportional risk increasing for example with the biological age (Demongeot 2009). Such an approach would be more realistic than the Mac Donald's one by taking into account the resistance of both vectors and hosts to infectious diseases, which is highly varying between young or elderly animals and humans; hence, it could be possible to give a better prediction of the efficacy of public health policies like vector eradication, vaccination, quarantine or other preventive actions in the different age classes of the populations of vectors and hosts.

10 Conclusion

We have considered in this paper some natural extensions of the classical Ross-McKendrick-Mac Donald approaches, in order to account for demographic and spatial dependencies of the contagion parameters on the host age and on the vector spread. Two examples have been presented, the first concerning the malaria

incidence with environmental dependency in Bankoumana, a locality of Sudanese savannah area in Mali, and the second concerning a retro-prediction of the medieval Black Death epidemics between 1348 and 1350 in Western Europe. Both examples show the interest of the introduction of space and age into the classical equations. In the future, some realistic examples (like Sexually Transmitted Diseases, STD) will be treated showing also the importance of the demography (the sexual relationships depending on the age of the partners) and of the socio-geography (conditioning the sexual behavior). Eventually, based on the knowledge of the new aerial routes (Khan et al. 2009), the study of the Black Death could also be revisited for the prediction of new possible plague pandemics from the Central Asia reservoir, with a viscosity vanishing no more on maritime but on aerial routes.

Acknowledgments We are indebted to L. Forest for his invaluable contribution to models, simulations and for his unforgettable friendship.

References

Abbas L, Demongeot J, Glade N (2009) Synchrony in reaction-diffusion models of morphogenesis: applications to curvature-dependent proliferation and zero-diffusion front waves. Philos Trans R Soc A 367:4829–4862

Balenghien T, Fouque F, Sabatier P, Bicout DJ (2006) Horse-, bird-, and human-seeking behavior and seasonal abundance of mosquitoes in a West West Nile virus focus of southern France. J Med Entomol 43:936–946

Barry S, Gualde N (2006) The biggest epidemics of history. L'Histoire 310:38–49

Baum TP, Pasqual N, Thuderoz F, Hierle V, Chaume D, Lefranc MP, Jouvin-Marche E, Marche P, Demongeot J (2004) IMGT/GeneInfo: enhancing V(D)J recombination database accessibility. Nucleic Acids Res 32:51–54

Beaudoin D, Lakhal-Chaieb L (2008) Archimedean copula model selection under dependent truncation. Stat Med 27:4440–4454

Benedictow OJ (2004) The black death 1346–1353: the complete history. Boydell Press, Woodbridge

Bernoulli D (1760) Essai d'une nouvelle analyse de la mortalité causée par la petite vérole, et des avantages del'inoculation pour la prévenir. Mém Acad Roy Sci, Paris

Bicout DJ, Sabatier P (2004) Mapping rift valley fever vectors and prevalence using rainfall variations. Vector-Borne Zoonotic Dis 4:33–42

Bicout DJ, Chalvet-Monfray K, Sabatier P (2002) Infection persistence time of Aedes breeding habitats. Physica A Stat Mech Appl 305:597–603

Brandenburg A, Multamaki T (2004) How long can left and right handed life forms coexist? Int J Astrobiol 3:209–219

Brossollet J, Mollaret H (1994) Pourquoi la peste ? Le rat, la puce et le bubon. Gallimard, Paris

Brouhns N, Denuit M (2001) Risque de longévité et rente viagère. Institut de Statistique Université Catholique, Louvain, Discussion Paper 0137

Cantor NF (2001) In the wake of the plague: the black death and the world it made. Free Press, New York

Carpentier E (1993) Une ville devant la peste, Orvieto et la peste noire de 1348. De Boeck Université, Bruxelles

Christakos G, Olea RA, Serre ML, Yu HL, Wang LL (2005) Interdisciplinary public health reasoning and epidemic modelling: the case of black death. Springer, Berlin

Cohn SK Jr (2002) The black death: end of a paradigm. Am Hist Rev 107:1–54

Cooke RM, Morales-Napoles O (2006) Competing risk and the cox proportional hazard model. J Stat Plan Inference 136:1621–1637

D'Alembert J (1761) Opuscules Mathématiques. David, Paris

de Magny GC, Paroissin C, Cazelles B, de Lara M, Delmas JF, Guégan JF (2005) Modeling environmental impacts of plankton reservoirs on cholera population dynamics. Esaim 14:156–173

Demetrius L (1979) Relations between demographic parameters. Demography 16:329–338

Demongeot J (1983) Thesis. Université J. Fourier, Grenoble
Demongeot J (2009) Biological boundaries and biological age. Acta Biotheor 57:397–419
Demongeot J, Demetrius L (1989) La dérive démographique et la sélection naturelle: Etude empirique de la France (1850–1965). Population 2:231–248
Demongeot J, Fricot J (1986) Random fields and renewal potentials. NATO ASI Serie F 20:71–84
Demongeot J, Glade N, Forest L (2007a) Liénard systems and potential-Hamiltonian decomposition. I Methodology. Comptes Rendus Mathématique 344:121–126
Demongeot J, Glade N, Forest L (2007b) Liénard systems and potential-Hamiltonian decomposition. II Algorithm. Comptes Rendus Mathématique 344:191–194
Demongeot J, Glade N, Moreira A, Vial L (2009) RNA relics and origin of life. Int J Mol Sci 10:3420–3441
Depinay JMO, Mbogo CM, Killeen G, Knols B, Beier J, Carlson J, Dusho J, Billingsley P, Mwambi H, Githure J, Toure AM, McKenzie FE (2004) A simulation model of African Anopheles ecology and population dynamics for the analysis of malaria transmission. Malaria J 3:29
Dietz K, Heesterbeek JAP (2000) Bernoulli was ahead of modern epidemiology. Nature 408:513
Dietz K, Heesterbeek JAP (2002) Daniel Bernoulli's epidemiological model revisited. Math Biosci 180:1–21
Doliger C (2006) Démographie, fécondité et croissance économique en France. Thesis Université Louis Pasteur, Strasbourg
Doumbo OK (2005) It takes a village: medical research and ethics in Mali. Science 307:679–681
Drancourt M, Aboudharam G, Signoli M, Dutour O, Raoult D (1998) Detection of 400-year-old Yersinia pestis DNA in human dental pulp: an approach to the diagnosis of ancient septicemia. Proc Natl Acad Sci USA 95:2637–12640
Dutertre J (1976) Étude d'un modèle épidémiologique appliqué au paludisme. Ann Soc Belge Méd Trop 56:127–141
Eckert EA (2000) The black death and the transformation of the West. Bull Hist Med 74:356–357
Fisher RA (1937) The wave of advance of advantageous genes. Ann Eugenics 7:353–369
Forest L, Glade N, Demongeot J (2007) Liénard systems and potential-Hamiltonian decomposition. Applications. C R Acad Sci Biol 330:97–106
Gani R, Leach S (2004) Epidemiologic determinants for modelling pneumonic plague outbreaks. Emerg Infect Dis 10:608–614
Gaudart J, Giorgi R, Poudiougou B, Ranque S, Doumbo OK, Demongeot J (2007) Spatial cluster detection: principle and application of different general methods. Rev Epidemiol Santé Publique 55:297–306
Gaudart J, Touré O, Dessay N, Dicko AL, Ranque S, Forest L, Demongeot J, Doumbo OK (2009) Modelling malaria incidence with environmental dependency in a locality of Sudanese savannah area, Mali. Malar J 8:61
Gaudart J, Ghassani M, Mintsa J, Waku J, Rachdi M, Doumbo OK, Demongeot J (2010) Demographic and spatial factors as causes of an epidemic spread, the copule approach. Application to the retro-prediction of the black death epidemy of 1346. In: IEEE AINA' 10 & BLSMC' 10. IEEE Press, Piscataway, pp 751–758
Glade N, Forest L, Demongeot J (2007) Liénard systems and potential-Hamiltonian decomposition. III Applications in biology. Comptes Rendus Mathématique 344:253–258
Horie M, Honda T, Suzuki Y, Kobayashi Y, Daito T, Oshida T, Ikuta K, Jern P, Gojobori T, Coffin JM, Tomonaga K (2010) Endogenous non-retroviral RNA virus elements in mammalian genomes. Nature 463:84–88
Horrox R (1994) The black death. Manchester University Press, Manchester
Huang J, Walker ED, Otienoburu PE, Amimo F, Vulule J, Miller JR (2006) Laboratory tests of oviposition by the african malaria mosquito, Anopheles gambiae, on dark soil as influenced by presence or absence of vegetation. Malaria J 5:88
Kelly J (2005) The great mortality: an intimate history of the black death, the most devastating plague of all time. Harper Collins, New York
Kermack WO, McKendrick AG (1932) Contributions to the mathematical theory of epidemics. II. The problem of endemicity. Proc R Soc Lond A 138:55–83
Kermack WO, McKendrick AG (1933) Contributions to the mathematical theory of epidemics. III. Further studies of the problem of endemicity. Proc R Soc Lond A 141:94–122

Khan K, Arino J, Hu W, Raposo J, Sears J, Calderon F, Heidebrecht C, Macdonald M, Liauw J, Chan A, Gardam M (2009) Spread of a novel Influenza A (H1N1) virus via global airline transportation. N Engl J Med 361:212–214

L'Épine GJ (1764) Rapport de six des douze commissaires (contre l'inoculation). Quillau, Paris, pp 40–43

La peste humaine en 1997 (1999) Relevé Epidémiologique Hebdomadaire OMS 74, 340–344

Lambert JH (1772) Beiträge zum Gebrauche der Mathematik und deren Anwendung". Dritter Theil, Berlin

Leslie PH (1945) On the use of matrices in certain population mathematics. Biometrika 33:183–212

Mac Donald G (1957) The epidemiology and control of malaria. Oxford University Press, London

Maupertuis PL Moreau de (1745, reed. 1965) Vénus physique, in Oeuvres. Georg Olms, Hildesheim

May N (1770) Impartial remarks on the Suttonian method of inoculation. Tilley, Wheble & Brown, London

May RM, Anderson RM (1984) Spatial heterogeneity and the design of immunization programs. Math Biosci 72:83–111

McKendrick AG (1925) Applications of mathematics to medical problems. Proc Edinburgh Math Soc 44:1–34

Mendez V, Fort J, Rotstein HG, Fedotov S (2003) Speed of reaction-diffusion fronts in spatially heterogeneous media. Phys Rev E 68:041105

Mischlewski A (1995) Un ordre hospitalier au Moyen Âge. Les chanoines réguliers de Saint-Antoine en Viennois. PUG, Grenoble

Mocellin G, Experton I (1992) Saint Antoine et l'Ordre des Antonins aux XVIIème et XVIIIème siècles. Ed. Musée, St-Antoine l'Abbaye

Mocellin-Spicuzza G (2002) Chroniques d'une abbaye au Moyen-Age. Guérir l'âme et le corps. Ed. Musée, Saint-Antoine l'Abbaye

Murray JA (1763) Fata variolarum insitionis in Suecia. Doctoral dissertation Universtiy Göttingen, Göttingen

Murray JD (2002) Mathematical biology I & II. Springer, Berlin

Ndiaye PI, Bicout DJ, Mondet B, Sabatier P (2006) Rainfall triggered dynamics of Aedes mosquito aggressiveness. J Theor Biol 243:222–229

Neerinckx SB, Peterson AT, Gulinck H, Deckers J, Leirs H (2008) Geographic distribution and ecological niche of plague in sub-Saharan Africa. Int J Health Geogr 7:54

Orent W (2001) Will the black death return? Discover 22:1–10

Orent W (2004) Plague: the mysterious past and mystifying furture of the world's most dangerous disease. Free Press, New York

Porphyre T, Bicout DJ, Sabatier P (2004) Modelling the abundance of mosquito vectors versus flooding dynamics. Ecol Modell 183:173–181

Porte M (1994) Passion des formes. A René Thom. ENS Editions, Paris

Prentice MB, Rahalison L (2007) Plague. Lancet 369:1196–1207

Raoult D, Aboudharam G, Crubézy E, Larrouy G, Ludes B, Drancourt M (2000) Molecular identification of 'Suicide PCR' of *Yersinia pestis* as the agent of medieval black death. Proc Natl Acad Sci USA 97:12800–12803

Renouard Y (1948) Conséquences et intérêt démographiques de la Peste noire de 1348. Population 3:459–466

Ross R (1916) An application of the theory of probabilities to the study of a priori pathometry. Part I. Proc R Soc Lond A 92:204–230

Russell JC (1948) British medieval population. Univ. of New Mexico, Albuquerque

Russell JC (1972) Population in Europe. In: Cipolla CM (ed) The Fontana economic history of Europe, vol. I, the middle ages. Collins/Fontana, Glasgow, pp 25–71

Scott S, Duncan C (2004) Return of the black death: the world's greatest serial killer West Sussex. Wiley, New York

Stenseth NC, Atshabar BB, Begon M, Belmain SR, Bertherat E, Carniel E, Gage KL, Leirs H, Rahalison L (2008) Plague: past, present, and future. PLOS Med 5:e3

Thom R (1972) Stabilité structurelle et Morphogenèse. Benjamin, New York

Thuderoz F, Simonet MA, Hansen O, Dariz A, Baum TP, Hierle V, Demongeot J, Marche PN, Jouvin-Marche E (2010) From the TCRAD rearrangement quantification to the computational simulation of the locus behavior. PloS Comp Biol 6:e1000682

Trembley J (1796) Recherches sur la mortalité de la petite vérole. Mém Acad Roy Sci, Paris

Usher MB (1969) A matrix model for forest management. Biometrics 25:309–315

Villani G (2001) Florence, 1336–38, the chronicle of Giovanni Villani. In: Medieval trade in the mediterranean world, Lopez, R.S. & I.W. Raymond Trads., Columbia Un. Press, New York
Wheelis M (2002) Biological warfare at the 1346 Siege of Caffa. Emerg Infect Dis 8:971–975
WHO (1999) La peste humaine en 1997. Relevé Epidémiologique Hebdomadaire OMS 74:340–344
Wood JW (2003) The temporal dynamics of the fourteenth-century black death: new evidence from english ecclesiastical records. Hum Biol 75:427–448
Zeeman EC (1993) Controversy in science: on the ideas of Daniel Bernoulli and René Thom. Nieuw Arch Wisk 11:257
Zhang SY, Yu L, Daszak P (2008) EcoHealth and the black death in the year of the rat. Ecohealth 5:99–100